Surface Chemistry

DOI: 10.1002/anie.200702444

Palladium Monomers, Dimers, and Trimers on the MgO(001) Surface Viewed Individually**

Martin Sterrer, Thomas Risse, Livia Giordano, Markus Heyde, Niklas Nilius, Hans-Peter Rust, Gianfranco Pacchioni, and Hans-Joachim Freund*

It has long been known that the size of metal clusters can tremendously influence the catalytic activity of oxide-supported metal catalysts.[1] To understand the physical and chemical principles that give rise to this effect, as well as to establish a relation between the structure and size of the catalyst particles and their reactivity, a detailed knowledge about the size-dependent geometrical properties and the corresponding electronic features is necessary.[2–4] This information is of particular importance for very small particles, constituting only a few atoms, whose properties cannot be predicted by scaling laws. Recently, progress has been made in studying the electronic and geometric properties of supported metal particles only a few atoms in size by depositing gas-phase selected clusters on oxide surfaces.[5–8] However, the size and shape of the small clusters on the surface, as well as the nature of their adsorption site—regular surface sites or defects—often remains unclear, especially if non-imaging techniques are applied. Therefore, most of our knowledge of oxide-supported metal atoms and small clusters comes from theoretical studies. Herein, we use low-temperature scanning tunneling microscopy (STM) to investigate experimentally the smallest oxide-supported metal particles, including the exact determination of their stoichiometry and adsorption sites, using Pd/MgO as a model system.

The Pd/MgO system is particularly interesting since MgO-supported palladium nanoparticles are among the best studied model catalysts in terms of cluster growth and structure,[9–12] as well as catalytic activity, which has been found even in the single-atom regime.[6,13,14] Although experimental techniques have yielded valuable information on the structure of MgO-supported palladium nanoparticles,[15] the properties of single atoms and small clusters, such as nucleation sites, bonding mechanism, geometric structure, and diffusion, are only available from theory.[16–23] Herein we report the geometry, adsorption sites, and electronic states of small Pd particles (Pd_1, Pd_2, Pd_3) adsorbed on regular surface sites of MgO thin films. The manipulation and investigation capabilities of STM are combined with information obtained from density functional theory (DFT), to provide a detailed experimental and theoretical description of the structural and electronic properties of the particles.

An STM image of the surface of a three-monolayer thin MgO/Ag(001) film acquired after deposition of Pd at a substrate temperature of 5–10 K is shown in Figure 1 (see the Supporting Information for experimental details), together with an atomically resolved image representing one ionic sublattice of the MgO surface. The majority of the deposited Pd is adsorbed as single atoms and only a small fraction forms aggregates, seen as the brighter spots in Figure 1.[24]

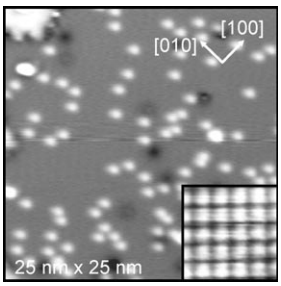

Figure 1. STM image of Pd adatoms on a 3-monolayer-thin MgO film ($T = 5$ K, $V_S = +0.5$ V, $i_t = 10$ pA). The inset shows an atomically resolved image (1.5 nm × 1.5 nm, $V_S = 15$ mV, $i_t = 7$ nA) of the surface of a thin MgO film (only one ionic sublattice is resolved).

In Figure 2a a small area of the MgO surface with adsorbed Pd adatoms (**1**–**4**) and a small aggregate (**5**), is shown. For better visualization, this image has been inverted and the height scale has been adjusted to reduce the apparent size of the Pd adatoms (Figure 2b). Superposition of the ionic sublattice extracted from atomically resolved images of the MgO surface (inset in Figure 1) reveals that all the Pd adatoms are located on the same type of site on the superimposed lattice (Figure 2b). A voltage pulse (typically 1.5–2 V) applied with the STM tip near the location of the Pd adatom **1** induced a hopping to the new position (**1***), which corresponds again to an equivalent lattice site (Figure 2c and d). This result indicates the existence of only one favorable adsorption site for Pd on this surface, in contrast to Au atoms adsorbed on MgO films of the same thickness, where several different adsorption sites are occupied.[25] A direct assignment of the Pd adsorption site (Mg or O) cannot be made based on

[*] Dr. M. Sterrer, Dr. T. Risse, Dr. M. Heyde, Dr. N. Nilius, Dr. H.-P. Rust, Prof. Dr. H.-J. Freund
Fritz-Haber-Institut der Max-Planck-Gesellschaft
Abteilung Chemische Physik
Faradayweg 4–6, 14195 Berlin (Germany)
Fax: (+49) 30-8413-4105
E-mail: sterrer@fhi-berlin.mpg.de
Dr. L. Giordano, Prof. Dr. G. Pacchioni
Universitá di Milano-Bicocca
Dipartimento di Scienzia dei Materiali
via R. Cozzi 53, 20125 Milano (Italy)

[**] This work has been supported by the European Union through STREP GSOMEN, COST D41, and NoE IDECAT. Further support by the Fonds der Chemischen Industrie is acknowledged.

Supporting information for this article is available on the WWW under http://www.angewandte.org or from the author.

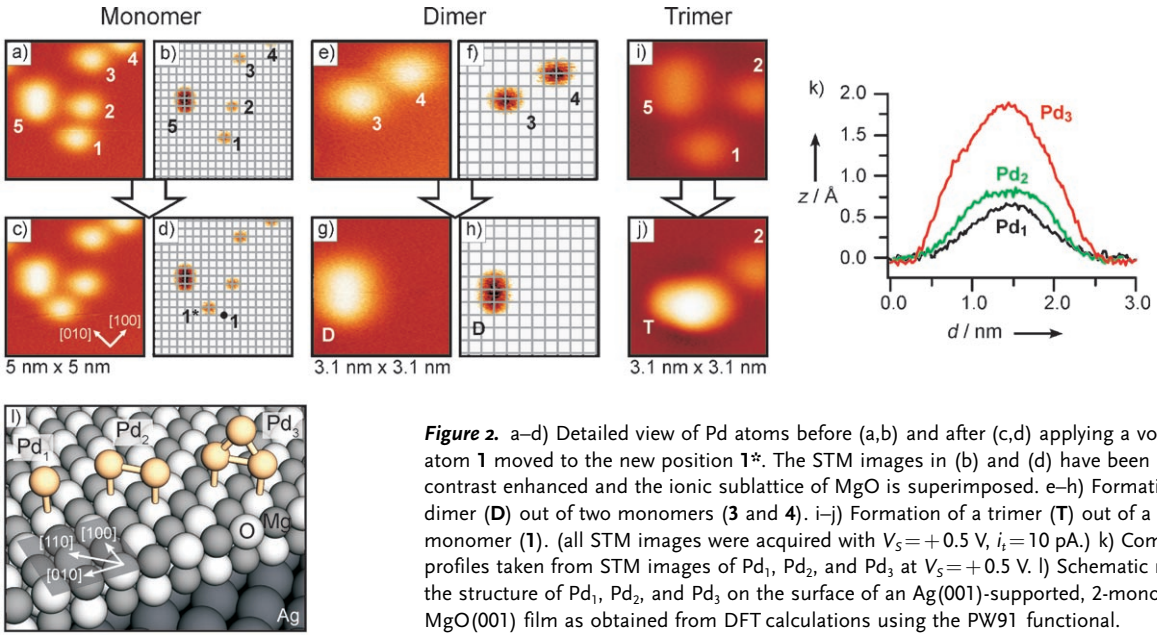

Figure 2. a–d) Detailed view of Pd atoms before (a,b) and after (c,d) applying a voltage pulse. Pd atom **1** moved to the new position **1***. The STM images in (b) and (d) have been inverted and contrast enhanced and the ionic sublattice of MgO is superimposed. e–h) Formation of a Pd dimer (**D**) out of two monomers (**3** and **4**). i–j) Formation of a trimer (**T**) out of a dimer (**5**) and a monomer (**1**). (all STM images were acquired with $V_S = +0.5$ V, $i_t = 10$ pA.) k) Comparison of line profiles taken from STM images of Pd_1, Pd_2, and Pd_3 at $V_S = +0.5$ V. l) Schematic representation of the structure of Pd_1, Pd_2, and Pd_3 on the surface of an Ag(001)-supported, 2-monolayrer-thin MgO(001) film as obtained from DFT calculations using the PW91 functional.

this experiment. However, DFT calculations show that on bulk MgO(001) the highest binding energy is found for Pd on top of the oxygen ions of the substrate.[26] This result is what we also find from plane-wave DFT calculations (PW91, see Supporting Information for more details) for the adsorption of Pd on a thin MgO film supported by Ag(001) (Figure 2l). Therefore, these experiments provide strong support for the theoretical prediction that Pd adsorbs on top of the oxide anions. The calculations also show that Pd behaves in a similar way when deposited on MgO thin films or on bulk MgO.

During scanning at higher sample bias V_S (typically 1.5–2 V), a Pd dimer (**D**) spontaneously formed from the two monomers **3** and **4** (Figures 2e–h). Similarly, a Pd trimer (**T**) was produced from a dimer **5** and a monomer **1** (Figure 2i,j). The elongated appearance in Figure 2g suggests that Pd_2 is lying flat on the surface. Given that the Pd monomers are located on top of oxygen ions (Figure 2f), the adsorption of Pd_2 along the oxygen-⟨110⟩ rows of the MgO substrate can readily be deduced (Figure 2h, see also the dimer **5** in Figure 2b), in agreement with the theoretical prediction of the energetically most favorable adsorption geometry of Pd_2 on MgO(100) (Figure 2l).[16] However, from the analysis of Figure 2h, the Pd dimer seems not to be located directly on top of two oxygen ions, but is slightly displaced. This occurrence could either be due to an experimental uncertainty, or the result of a slight lateral displacement along the [110] direction. Corresponding calculations for Pd_2 adsorption on thin MgO/Ag(001) films predict displacements of 0.2–0.3 Å to be almost barrierless.

Like Pd_2, Pd_3 is also elongated along the ⟨110⟩ directions (Figure 2j), and, under the given tunneling conditions, appears higher and slightly larger than Pd_1 and Pd_2, as shown in the line profiles in Figure 2k. This appearance excludes the presence of Pd_3 clusters lying parallel to the surface plane (i.e. flat-lying triangle) because of the expected deviation from an elongated signature. However, the discrimination between a linear configuration (Pd_3 chain) and a triangular one oriented perpendicular to the surface is not possible. The increased apparent height of the cluster hints, however, towards the triangular conformation. This notion is corroborated by theoretical calculations predicting perpendicularly oriented Pd_3 triangles (Figure 2l) to be the most stable conformation.[27]

An interpretation of the cluster geometry solely based on the apparent height z and the STM appearance of the Pd particles has to be treated with caution. On the one hand, z is affected by the electronic states of the clusters, and on the other hand, the appearance might be influenced by the orbital symmetry of the states that are probed at particular bias voltages V_S. Concerning the latter point, we did not observe any change of the cluster shape on changing V_S. However, the apparent height of the different Pd particles varies considerably as a function of applied V_S (Figure 3a). An enhancement of z in the constant-current imaging mode reflects an increase in tunneling probability when an electronic state of the cluster is probed. The opening of an extra tunneling channel in the electronic states leads to a step in the z-V_S curves (Figure 3a). Depending on the tunneling polarity, these states are either filled or empty, whereby positive polarity corresponds to tunneling into empty states and negative sample bias tunneling from the filled states. Therefore, valuable information about the electronic structure of the Pd particles can be deduced from analyzing the z-V_S dependence.

From Figure 3a it can be concluded that both Pd_1 and Pd_2 exhibit an empty state between 1 eV and 1.5 eV above the Fermi energy E_F, with that of Pd_2 slightly shifted towards lower energies. No feature could be detected in the filled states region (the V_S range for this analysis was limited to max. ±1.5 V because of instabilities of the small Pd particles at higher tunneling voltages). For Pd_3 a filled state is detected about 1.3 eV below E_F, as deduced from the increase in

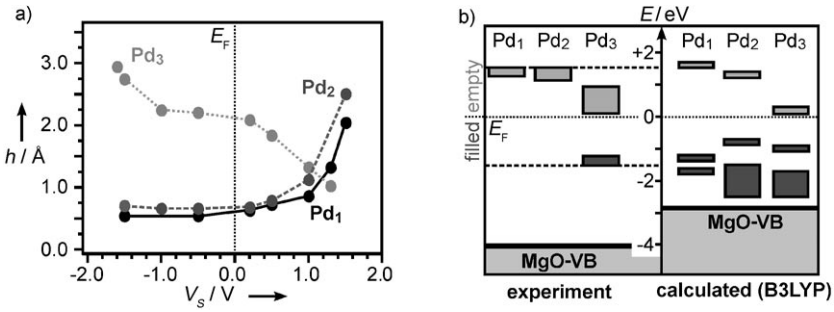

Figure 3. a) Bias voltage (V_S) dependence of the apparent height z for a Pd monomer (Pd_1), dimer (Pd_2), and trimer (Pd_3). b) Comparison of the experimentally detected and calculated (using the B3LYP functional) energies of filled (black) and empty (gray) states of Pd_1, Pd_2, and Pd_3 on the MgO surface, referenced to the Fermi energy (E_F). In the experiment, the energy range was limited between 1.5 eV above and below E_F (dashed horizontal lines; VB = valence band).

apparent height in this V_S range. In addition, a drastic decrease of z corresponding to a negative differential conductance is found above E_F. This behavior points to the existence of an unoccupied state located close to E_F which dominates the current at low positive bias but looses influence at higher bias. The decreasing apparent height with increasing positive bias indicates the absence of unoccupied states in the Pd trimer in the energy window between 0.5–1.5 eV above E_F, causing an approach of the tip to the sample surface to maintain a constant tunnel current. The gap between highest occupied and lowest unoccupied states in Pd_3 is about 1.5 eV.

The analysis of the z-V_S dependence indicates that the electronic properties of the monomer and dimer are quite similar while that of the trimer is significantly altered. This observation does not fit into the simple picture of a weak metal–oxide interaction and a rather strong metal–metal interaction, because a more severe difference between monomer and dimer would have been anticipated.

To corroborate the experimental findings on the energetic position of the Pd filled and empty states, we compared the experimental results with DFT embedded cluster calculations using the B3LYP hybrid functional and localized basis sets. The reason for using B3LYP is that it provides, in comparison to the standard plane-wave approach with the PW91 functional, a more accurate description of the energy gap of insulators, such as MgO,[28] and of the position of the Pd filled and empty states with respect to the MgO valence band (VB) edge. The results of the B3LYP calculations are compiled in Figure 3b, with the position of the states aligned with respect to E_F. The comparison between experimental and theoretical results yields qualitatively similar trends for the unoccupied orbitals of Pd_1, Pd_2, and Pd_3. For Pd_1/MgO the empty state probed in experiment corresponds to the lowest unoccupied level, which is of exclusively 5s character. The calculated HOMO–LUMO gap is about 2.9 eV. Given that the computed energies are slightly underestimated, this result explains why the Pd_1 filled state is not observed in the V_S range accessible in the experiments.

The empty state of Pd_2 has s character and its energetic position is very similar to that of Pd_1, in accordance with the experimental findings (Figure 3b). This unexpected behavior can be rationalized based on the theoretical results: the calculated Pd–Pd bond in the supported dimer is 2.8 Å and thus significantly elongated with respect to the gas-phase dimer, 2.5 Å. The energy gain associated to the formation of MgO-supported Pd_2 from two Pd_1 adatoms is only 0.5 eV.[21] Thus, the metal–metal bond in the supported dimer is rather weak and, consequently, the electronic properties of Pd_2 are largely dominated by those of single atoms. In particular, the HOMO–LUMO gap of Pd_2, calculated to be 2.1 eV, is large, although less than in the monomer (2.9 eV). Note that the probability for detecting filled electronic d states of small transition-metal clusters by STM could be rather small, this is either because of ionization of the cluster resulting from small tunneling rates of electrons through the insulating thin film, or because of insufficient overlap between the wavefunctions of cluster and tip. The presence of filled states for Pd_1 and Pd_2 in the V_S range from 0 to −1.5 eV can, therefore, not be completely excluded.

In contrast to Pd_1 and Pd_2, the gap between filled and empty states is considerably reduced for Pd_3—1.5 eV in experiment and 1.1 eV in the calculations—indicative for enhanced metal–metal bonding. Both the HOMO and the LUMO of Pd_3 have mixed 4d and 5s hybrid character. The LUMO + 1 is separated from the LUMO by 1.9 eV, which explains the experimentally observed decrease of the apparent height of Pd_3 with increasing bias voltage up to 1.5 V above E_F. Note that this qualitative one-electron picture is corroborated by more elaborate calculations which include many electron effects. The close agreement between experimentally deduced and calculated electronic properties of the Pd particles supports the results concerning their geometric structure as inferred from the STM images in Figure 2. This situation provides strong evidence that the artificially created Pd particles exhibit the equilibrium structures for adsorption on a regular, defect-free MgO surface as calculated from DFT.

There are several aspects worth highlighting at this point: first, the STM results provide the first experiments to characterize the geometric and electronic structure of metal clusters on oxide surfaces with direct control on the cluster stoichiometry. To this end, these are benchmark studies for theoretical calculations. Second, STM manipulation of metal atoms already has a long tradition,[29–32] however, on oxide surfaces only single metal adatoms or self-assembled structures have been investigated.[33–35] The study presented herein provides a first step towards using STM to assemble small metal clusters that exhibit theoretically predicted equilibrium structures on oxide surfaces. In the future, this could provide relevant information on, for example, diffusion of selected clusters, trapping at different kinds of defects, or agglomeration.

In summary, we have shown for Pd/MgO(001) as a model system that by manipulation of adatoms with a STM tip small

metal particles adsorbed on oxide surfaces can be created and subsequently characterized with experimental control over the stoichiometry and the adsorption sites of the particles. The comparison of information from experiment and from DFT calculations confirms that the artificially created Pd particles exhibit geometric and electronic properties expected for the energetically most stable configurations of Pd particles with the same stoichiometry adsorbed on regular sites of the MgO(001) surface.

Received: June 5, 2007
Published online: October 8, 2007

Keywords: ab initio calculations · cluster compounds · magnesium oxide · palladium · scanning probe microscopy

[1] M. Che, C. O. Bennet, *Adv. Catal.* **1989**, *20*, 153.
[2] C. T. Campbell, *Surf. Sci. Rep.* **1997**, *27*, 1.
[3] C. R. Henry, *Surf. Sci. Rep.* **1998**, *31*, 231.
[4] M. Bäumer, H.-J. Freund, *Prog. Surf. Sci.* **1999**, *61*, 127.
[5] M. H. Schaffner, F. Patthey, W.-D. Schneider, *Eur. Phys. J. D* **1999**, *9*, 609.
[6] S. Abbet, A. Sanchez, U. Heiz, W.-D. Schneider, A. M. Ferrari, G. Pacchioni, N. Rösch, *J. Am. Chem. Soc.* **2000**, *122*, 3453.
[7] L. Benz, X. Tong, P. Kemper, Y. Lilach, A. Kolmakov, H. Metiu, M. T. Bowers, S. K. Buratto, *J. Chem. Phys.* **2005**, *122*, 081102.
[8] X. Tong, L. Benz, P. Kemper, H. Metiu, M. T. Bowers, S. K. Buratto, *J. Am. Chem. Soc.* **2005**, *127*, 13516.
[9] C. Duriez, C. R. Henry, C. Chapon, *Surf. Sci.* **1991**, *253*, 190.
[10] G. Renaud, A. Barbier, O. Robach, *Phys. Rev. B* **1999**, *60*, 5872.
[11] G. Haas, A. Menck, H. Brune, J. V. Barth, J. A. Venables, K. Kern, *Phys. Rev. B* **2000**, *61*, 11105.
[12] C. Xu, W. S. Oh, G. Liu, D. Y. Kim, D. W. Goodman, *J. Vac. Sci. Technol. A* **1997**, *15*, 1261.
[13] C. Becker, C. R. Henry, *Surf. Sci.* **1996**, *352*, 457.
[14] A. S. Wörz, K. Judai, S. Abbet, U. Heiz, *J. Am. Chem. Soc.* **2003**, *125*, 7964.
[15] C. R. Henry, *Prog. Surf. Sci.* **2005**, *80*, 92.
[16] A. M. Ferrari, C. Y. Xiao, K. M. Neyman, G. Pacchioni, N. Rösch, *Phys. Chem. Chem. Phys.* **1999**, *1*, 4655.
[17] A. V. Matveev, K. M. Neyman, G. Pacchioni, N. Rösch, *Chem. Phys. Lett.* **1999**, *299*, 603.
[18] L. Giordano, J. Goniakowski, G. Pacchioni, *Phys. Rev. B* **2001**, *64*, 075417.
[19] V. A. Nasluzov, V. V. Rivanenkov, A. B. Gordienko, K. M. Neyman, U. Birkenheuer, N. Rösch, *J. Chem. Phys.* **2001**, *115*, 8157.
[20] A. Bogicevic, D. R. Jennison, *Surf. Sci.* **2002**, *515*, L481.
[21] L. Giordano, C. Di Valentin, J. Goniakowski, G. Pacchioni, *Phys. Rev. Lett.* **2004**, *92*, 096105.
[22] G. Barcaro, A. Fortunelli, F. Nita, R. Ferrando, *Phys. Rev. Lett.* **2005**, *95*, 246103.
[23] L. J. Xu, G. Henkelman, C. T. Campbell, H. Jonsson, *Phys. Rev. Lett.* **2005**, *95*, 146103.
[24] M. Sterrer, T. Risse, U. M. Pozzoni, L. Giordano, M. Heyde, H.-P. Rust, G. Pacchioni, H.-J. Freund, *Phys. Rev. Lett.* **2007**, *98*, 096107.
[25] M. Sterrer, T. Risse, M. Heyde, H.-P. Rust, H.-J. Freund, *Phys. Rev. Lett.* **2007**, *98*, 206103.
[26] I. Yudanov, G. Pacchioni, K. Neyman, N. Rösch, *J. Phys. Chem. B* **1997**, *101*, 2786.
[27] L. Giordano, G. Pacchioni, *Surf. Sci.* **2005**, *575*, 197.
[28] J. Muscat, A. Wander, N. M. Harrison, *Chem. Phys. Lett.* **2001**, *342*, 397.
[29] M. F. Crommie, C. P. Lutz, D. M. Eigler, *Science* **1993**, *262*, 218.
[30] L. Bartels, G. Meyer, K.-H. Rieder, *Phys. Rev. Lett.* **1997**, *79*, 697.
[31] N. Nilius, T. M. Wallis, W. Ho, *Science* **2002**, *297*, 1853.
[32] C. F. Hirjibehedin, C. P. Lutz, A. J. Heinrich, *Science* **2006**, *312*, 1021.
[33] N. Nilius, T. M. Wallis, W. Ho, *Phys. Rev. Lett.* **2003**, *90*, 046808.
[34] N. Nilius, E. D. L. Rienks, H.-P. Rust, H.-J. Freund, *Phys. Rev. Lett.* **2005**, *95*, 066101.
[35] M. Kulawik, N. Nilius, H.-J. Freund, *Phys. Rev. Lett.* **2006**, *96*, 036103.

